

SAR11 clade microdiversity and activity during the early spring blooms off Kerguelen Island, Southern Ocean

Dinasquet Julie ^{1,2,*}, Landa Marine ^{1,3}, Obernosterer I. Ingrid ¹

¹ CNRS, Sorbonne Université, Laboratoire d'Océanographie Microbienne, LOMIC Banyuls-sur-Mer , France

² Marine Biology Research Division and Climate, Atmospheric Science & Physical Oceanography Department Scripps Institution of Oceanography San Diego California , USA

³ Sorbonne Université/Centre National de la Recherche Scientifique UMR7144, Adaptation et Diversité en Milieu Marin, Station Biologique de Roscoff Roscoff, France

* Corresponding author : Julie Dinasquet, email address : jdinasquet@ucsd.edu

Abstract :

The ecology of the SAR11 clade, the most abundant bacterial group in the ocean, has been intensively studied in temperate and tropical regions, but its distribution remains largely unexplored in the Southern Ocean. Through amplicon sequencing of the 16S rRNA gene, we assessed the contribution of the SAR11 clade to bacterial community composition in the naturally iron fertilized region off Kerguelen Island. We investigated the upper 300 m at seven sites located in early spring phytoplankton blooms and at one high-nutrient low-chlorophyll site. Despite pronounced vertical patterns of the bacterioplankton assemblages, the SAR11 clade had high relative abundances at all depths and sites, averaging 40% ($\pm 15\%$) of the total community relative abundance. Micro-autoradiography combined with CARD-FISH further revealed that the clade had an overall stable contribution (45%–60% in surface waters) to bacterial biomass production (determined by 3H-leucine incorporation) during different early bloom stages. The spatio-temporal partitioning of some of the SAR11 subclades suggests a niche specificity and periodic selection of different subclades in response to the fluctuating extreme conditions of the Southern Ocean. These observations improve our understanding of the ecology of the SAR11 clade and its implications in biogeochemical cycles in the rapidly changing Southern Ocean.

52 **Introduction**

53 The SAR11 clade of the Alphaproteobacteria is one of the most abundant bacterioplankton in
54 marine ecosystems (Morris *et al.*, 2002; Carlson *et al.*, 2009; Eiler *et al.*, 2009) representing 25% or
55 more of the total bacterial cells in seawater worldwide (Giebel *et al.*, 2009; Brown *et al.*, 2012;
56 Sunagawa *et al.*, 2015; Ortmann and Santos, 2016). Since its first discovery (Giovannoni *et al.*, 1990),
57 the clade's spatial, vertical and seasonal patterns and links to ecosystem variables have been
58 extensively studied and described (e.g. Carlson *et al.*, 2009; Eiler *et al.*, 2009; Brown *et al.*, 2012;
59 Morris *et al.*, 2012; Vergin *et al.*, 2013; Salter *et al.*, 2014; Thrash *et al.*, 2014; Ortmann and Santos,
60 2016). Conserved traits such as small cell size, small streamlined genomes, simplified regulatory
61 systems, or efficient energy acquisition strategies seem to make members of this clade steady
62 competitors that thrive in the minimal conditions provided by oligotrophic marine waters, and likely
63 explain the clade's remarkable success throughout the world's oceans (reviewed in Giovannoni, 2017).
64 Their ubiquitous abundances and specialized, atypical carbon substrate utilization profiles make
65 SAR11 significant contributors to fluxes of carbon and other nutrients in the ocean (Giovannoni, 2017
66 and references therein). Beyond the existence of core characteristics shared by most members of the
67 clade, detailed examination of SAR11 microdiversity has revealed several phylogenetic subclades that
68 are consistently associated with specific environmental conditions (e.g. Field *et al.*, 1997; Carlson *et*
69 *al.*, 2009; Vergin *et al.*, 2013). These subclades seem to represent ecologically coherent populations or
70 ecotypes. Subclade-specific traits and metabolic needs have been identified and likely play an
71 important role in the ecological niche partitioning observed among the subclades (Grote *et al.*, 2012;
72 Thrash *et al.*, 2014; Tsementzi *et al.*, 2016; Haro-Moreno *et al.*, 2020).

73 There are, however, fewer studies on the distribution and ecology of SAR11 subclades in the Southern
74 Ocean (Brown *et al.*, 2012; Liu *et al.*, 2019; Haro-Moreno *et al.*, 2020; Sow *et al.*, 2022). The Southern
75 Ocean is the largest High Nutrient Low Chlorophyll (HNLC) region in the world, a result of the low
76 concentrations of the essential element iron (Fe) which limits primary production in surface waters
77 (Blain *et al.*, 2007; Pollard *et al.*, 2009). Concentrations of dissolved organic carbon (DOC) in Southern
78 Ocean surface waters are among the lowest of the global ocean (about 50 μ M; Hansell *et al.* 2010),
79 which in turns limits heterotrophic bacterial activity. Bacterial growth can also be co-limited by both Fe
80 and DOC (Church *et al.*, 2000; Obernosterer *et al.*, 2015). Thus, in this environment, metabolic
81 interactions shaping microbial communities are particularly complex, as diverse phytoplankton and
82 heterotrophic bacterial taxa compete for Fe (Fourquez *et al.*, 2016) while also relying on each other for
83 key resources such as labile organic carbon and vitamins (Bertrand *et al.*, 2007). Members of the
84 SAR11 clade are highly adapted to oligotrophic waters in which nutrient concentrations are low, but
85 they also have atypical metabolic requirements driven by genomic streamlining that hint at a strong
86 dependency on metabolites synthesized by co-occurring microbes. They have also been shown to be
87 dominant members of the microbial communities in other HNLC regions such as the Subarctic Pacific
88 and Equatorial Pacific (e.g. Jing *et al.*, 2013; West *et al.*, 2016). For these reasons, the Southern Ocean
89 provides an interesting environmental framework to investigate the activity and diversity of SAR11 and
90 can contribute unique insight into the ecology of this marine bacterial clade.

91 Previously published work showed that in the Kerguelen area of the Southern Ocean, SAR11
92 populations can be abundant members of bacterial communities. The SAR11 clade was most successful
93 in HNLC waters independent of season (West *et al.*, 2008; Landa *et al.*, 2016; Hernandez-Magana *et*
94 *al.*, 2021) where they also actively contribute to bacterial carbon uptake and cycling (Obernosterer *et*

95 *al.*, 2011; Fourquez *et al.*, 2016; Sun *et al.*, 2021). By contrast, in the naturally Fe fertilized waters off
96 the Kerguelen plateau (Blain *et al.*, 2007) the relative abundance of SAR11 revealed a pronounced
97 seasonal pattern, starting with high relative abundances in the early bloom stage, followed by a drastic
98 decrease after the spring phytoplankton bloom and an increase towards late summer (Liu *et al.*, 2020).
99 Whether or not different sublineages were found in HNLC waters and in the blooms or throughout the
100 water column has implications for understanding the lifestyle and specific traits of SAR11 bacteria in
101 these environments. In the present report, we follow up on the aforementioned studies and leverage the
102 rich existing sample set to provide a detailed analysis of SAR11 activity, sublineage diversity and
103 distribution patterns in this mosaic of phytoplankton blooms induced by natural Fe fertilization. Our
104 results indicate that SAR11 populations remained abundant and active throughout the water column.
105 Microdiversity analysis detected members from most known SAR11 sublineages and revealed distinct
106 community composition at depth and across bloom stations.

107
108

Results and discussion

The samples for the present study were collected in naturally Fe-fertilized and in HNLC waters off Kerguelen Island in early spring during the KEOPS2 cruise (Fig.S1). Concentrations of Chl *a*, bacterial abundance and bacterial heterotrophic production were overall higher in naturally Fe-fertilized mixed and intermediate waters as compared to the HNLC station R-2 (Table S1 and references within). However, among the Fe-fertilized sites, considerable variability in these biological parameters were observed (Table S1), reflecting spatial and temporal variability in the blooms development (Lasbleiz *et al.*, 2016) . By contrast, the major inorganic nutrients N and P, and DOC were similar across sites and characteristic for this region (Blain *et al.*, 2015; Tremblay *et al.*, 2015). In the present report, samples from eight stations and four sampled depths (20 to 300 m) were sorted into three water layers named mixed layer, intermediate layer and deep layer (Table S1), identified based on oceanographic parameters (Park *et al.*, 2014).

Figure 1

We assessed the contribution of SAR11 to bacterial community using 16S rDNA amplicon sequencing at all stations and depth layers (Fig. 1). Additionally, we used CARD-FISH for 3 distinct Fe-fertilized bloom stations (A3.2; F-L and E-5) and the HNLC site R-2 (Table 1). Sequencing analysis showed that OTUs of the SAR11 clade represented on average $41 \pm 13\%$ (and up to 62% in intermediate waters) of total sequences and were dominant at all stations down to 300 m regardless of the bloom regimes (Fig. 1). This observation expands our initial observations of generally high SAR11 relative abundances in surface waters (20 m) (Landa *et al.*, 2016). The contribution of the SAR11 clade to bulk bacterial abundance based on CARD-FISH counts varied between $44.3 \pm 4\%$ in HNLC waters and $33 \pm 10\%$ at the three Fe-fertilized bloom stations A3.2, F-L and E-5, in the mixed and intermediate

layers (Table 1). Both microscopic and molecular methods provided comparable values that are in line with previous studies showing SAR11 abundances between 20 and 55% of the total bacterial communities in the same study area (West *et al.*, 2008; Obernosterer *et al.*, 2011; Hernandez-Magana *et al.*, 2021) and in other regions of the Southern Ocean (Giebel *et al.*, 2009; Tada *et al.*, 2013). Both methods were generally in good agreement for most samples, however discrepancies between the two were observed in the deep-water samples (Table 1). The decrease in SAR11 relative abundances at 300 m compared to the mixed layer values was more pronounced for the CARD-FISH data than for the sequencing data. One limitation of the CARD-FISH approach is that cells with a low rRNA content are not always detected, while the PCR step required for 16S rRNA gene sequencing targets live, dormant or even dead cells. Another possible explanation for the observed differences between the two methods could be the existence of distinct deep SAR11 clades missed by the set of probes used in our study. This latter was likely not the case as our probes appeared to target all the subclades present.

Table 1

The success of SAR11 as the most abundant marine bacterial group suggests that they play an important role in organic matter fluxes. Here, micro-autoradiography combined with CARD-FISH showed that 11-84% of SAR11 cells were active in the upper 80 m (Table 1) and this fraction was generally lower below 150m. The average $48.2 \pm 15.6\%$ of total active cells as SAR11 in the upper 150 m, is similar to that observed previously in other, warmer oceanic regions, such as the North Atlantic and Mediterranean Sea where SAR11 contributed to 30-50% of the leucine-incorporating community (Malmstrom *et al.*, 2004; Malmstrom *et al.*, 2005; Laghdass *et al.*, 2012) and higher than observed in other regions of the Southern Ocean (Straza *et al.*, 2010; Tada *et al.*, 2013). The contribution of SAR11 to bulk leucine incorporation was slightly lower than expected from their

153 contribution to abundance (Figure 2), a trend often observed in other regions (e.g., Elifantz *et al.*, 2005;
154 Alonso-Saez and Gasol, 2007; Alonso-Saez *et al.*, 2008, Straza *et al.*, 2010). A possible explanation is
155 that SAR11 cells grow slower than other bacterial groups, and thus do not incorporate as much leucine
156 as faster growing taxa. Interestingly and despite this seemingly moderate activity level of the SAR11
157 group, the taxon accounted for most of the leucine incorporating cell population, particularly in upper
158 layers (Table 1). Overall, our data indicate that SAR11 are important contributors to carbon cycling
159 across the studied region at this time of the year as a result of high abundances and sustained activity
160 levels in various bloom conditions.

161 **Figure 2**

162 The present and previous studies (Giebel *et al.*, 2009) highlight SAR11 to be major community
163 members in non-productive Southern Ocean waters. Despite the differences in the environmental
164 setting among stations (Table S1, Lasbleiz *et al.*, 2016) the contribution of SAR11 to the total cells and
165 to active cells appeared to be relatively constant. This is likely due to their successful adaptation to
166 oligotrophic waters and to their capacity to take up efficiently organic substrates, among those some
167 phytoplankton derived metabolites, such as very labile volatile molecules (Sun *et al.*, 2011; Moore *et*
168 *al.*, 2020, 2022), while other taxa may favor high molecular weight DOM utilization (Malmstrom *et al.*,
169 2005) as reported during the present cruise (Fourquez *et al.*, 2016; Landa *et al.*, 2018). So far, no
170 known siderophores or heme uptake genes have been observed in SAR11 genomes (Hogle *et al.*, 2016),
171 suggesting that the success of SAR11 in these Fe-limited waters could further be due to other specific
172 strategies related to uptake, storage and utilization of this limiting micronutrient (Beier *et al.*, 2015;
173 Debeljak *et al.*, 2019; Sun *et al.*, 2021). Pelagibacteraceae utilize predominantly inorganic Fe (Fe^{3+} ,
174 Hopkinson and Barbeau 2012; Debeljak *et al.*, 2019); their metabolic activity is likely to be sustained

175 by the seasonally high concentrations of dissolved Fe prior to the phytoplankton bloom development
176 (Qu  rou   *et al.*, 2015). Using MICRO-CARD-FISH, it was indeed shown that SAR11 made up 25% of
177 the community taking up Fe in surface waters at the sites investigated during the same cruise (Fourquez
178 *et al.*, 2016).

179 **Figure 3**

180 SAR11 subclades distribution over the studied area and dynamics during the onset of the spring
181 bloom was further resolved to phylogenetic subclades partitioning. Overall, 47 OTUs were closely
182 related to Pelagibacterales at 99% identity (covering 64310 reads, Fig. 3). The phylogenetic
183 relationship between these OTUs and previously identified SAR11 subclasses (e.g. Field *et al.*, 1997;
184 Carlson *et al.*, 2009; Vergin *et al.*, 2013) showed that OTUs observed in this study separated between
185 six different known subclades. Most of our reads (80  6%) belonged to subclade Ia, which is the most
186 abundant and most studied SAR11 ecotype in the ocean (e.g. Giovannoni, 2017; Delmont *et al.*, 2019).
187 This cluster could be further separated in three subgroups (Fig. 3). The most abundant OTU in our
188 dataset (KEOPS-6089, Fig. 3) represented 15% of the total relative abundance of all bacterial OTUs
189 across all samples (on average 80% of all SAR11) and clustered in the Ia.1 group, with the first
190 cultivated member of the clade: Pelagibacter HTCC1062 (Rapp   *et al.*, 2002). Ia. is the only subclade
191 with Fe regulatory mechanisms for adaptation to Fe limitation (Smith *et al.*, 2010; Gr  te *et al.*, 2012).
192 Subclade Ia is also adapted to respond to phytoplankton derived one-carbon and volatile organic
193 compounds (Sun *et al.*, 2011; Halsey *et al.*, 2017; Moore *et al.*, 2020, 2022). Its capacity to efficiently
194 utilize inorganic Fe and organic substances, or its low requirements of each to maintain cellular
195 activity, may explain the success of this SAR11 Ia.1 clade in the region.

196 **Figure 4**

197 The SAR11 clades distribution as a function of depth showed that specific OTUs were more
198 represented in different depth layers (Fig. 4). More specifically, subclades Ia, IIIa and IV were
199 relatively more abundant in mixed and intermediate layers, while subclade Ib was more abundant in the
200 deep layers (Fig. 4.A). Subclade Ib has also been reported in epi- and bathypelagic waters in the Red
201 Sea (Jimenez-Infante *et al.*, 2017). At the Atlantic time series site BATS, subclade Ib is usually found
202 in mixed water in late spring and early summer, while Ic is found in deeper water (Vergin *et al.*, 2013;
203 Trash *et al.*, 2014). Here, subclade Ic also increased in deeper waters, which may be related to specific
204 adaptation to nutrient availability (Tsementzi *et al.*, 2016; Ruiz-Perez *et al.*, 2021). Subgroup Ia.3 was
205 more abundant in the deep layers, while Ia.1 and Ia.2 had higher relative abundances in mixed and
206 intermediate layers (Fig. 4.B). Ia.1 has been observed in colder surface coastal waters (Rappe *et al.*,
207 2002; Brown *et al.*, 2012; Grote *et al.*, 2012), and in other regions of the Southern Ocean (Haro-
208 Moreno *et al.*, 2020). Ia.3 has been reported in surface gyre and tropical waters (Brown *et al.*, 2012;
209 Grote *et al.*, 2012; Delmont *et al.*, 2019). Nevertheless, Ia.3 has also been observed in deep water of the
210 Red Sea (Ngugi and Stingl, 2012).

211 **Figure5**

212 The microdiversity of SAR11 subclades appeared more dynamic in surface waters (20m, Fig.
213 5), similar to the shift in overall surface bacterial community composition at the sites characterized by
214 different early bloom stages (Landa *et al.*, 2016). The different subclades showed evident patterns
215 throughout the water column, with a shift in lineage identity and abundances at 300 m, compared to
216 more similar mixed and intermediate layers (Fig. 4 and 5). This pronounced layer difference in
217 microdiversity might be linked to the specific water masses circulation in the Southern Ocean. This

218 could also explain the general differences in microdiversity at station F-L, which is closest to the Polar
219 Front and more influenced by Indian Ocean warmer waters.

220 SAR11 microdiversity also exhibited specific patterns linked to the bloom progression (Fig. 5).
221 For instance, subclade IV was most abundant in more advanced bloom stage stations (A3.2, E4W and
222 FL) where it probably benefited from specific relationships with phytoplankton cells (e.g. Becker *et al.*,
223 2019; Tucker *et al.*, 2021), such as public good secondary metabolites and volatile organic compounds
224 produced by the phytoplankton (e.g. Giovannoni, 2017). Conversely, subclades Ic and IIa seemed most
225 abundant in the non-bloom stations (R-2, HNLC station and E3, Fig. 5) with low organic carbon
226 concentration. The bi-polar distribution of subclade IIa in surface waters has been previously reported
227 (Kraemer *et al.*, 2019); its adaptation to cold waters may explain its relatively stable distribution in less
228 productive stations across the water column in the study area. Subclades Ia and Ib did not seem to
229 respond to bloom stages (Fig. 5), which showcases their ability to maintain their metabolism regardless
230 of conditions. Ia.2 appeared to be more abundant in the HNLC waters; this subgroup was the second
231 most abundant in the region and did not cluster with published reference sequences (Fig. 3), suggesting
232 that this group was locally adapted to less productive and Fe-limited waters of the Southern Ocean.

233

234 In conclusion, Pelagibacterales are highly adapted to the cold, organic carbon- and iron-limited
235 waters of the Southern Ocean, which is consistent with the clade's notorious ability to efficiently
236 harvest limiting resources. The spatio-temporal partitioning of some of the SAR11 subclades revealed
237 in this study followed observations made on niche specificity and periodic selection in other oceanic
238 regions.

239 Nevertheless, the contribution of SAR11 to leucine incorporation was relatively stable across sites
240 despite the variations in microdiversity, suggesting that subclades have a redundant impact on the
241 carbon cycle or that one stable clade Ia1 was responsible for the overall activity. Investigating the
242 metabolic potential of these SAR11 subclades are key to better understand the underlying mechanisms
243 for their spatial distributions, and to further understand their evolution and ecological adaptation to the
244 extreme conditions of the Southern Ocean, where they contribute substantially to the bacterial biomass
245 and production and probably to other microbially mediated fluxes.

246

247

248 **Acknowledgments**

249 We thank S. Blain, the PI of the KEOPS2 project, for providing us the opportunity to participate to this
250 cruise, the chief scientist B. Quéguiner, the captain Bernard Lassiette and the crew of the R/V Marion
251 Dufresne for their enthusiasm and help aboard. This work was supported by the French Research
252 program of the INSU-CNRS LEFE-CYBER (Les enveloppes fluides et l'environnement –Cycles
253 biogéochimiques, environnement et ressources), the French ANR (Agence Nationale de la Recherche,
254 SIMI-6 program), the French CNES (Centre National d'Etudes Spatiales) and the French Polar Institute
255 IPEV (Institut Polaire Paul-Emile Victor). JD was supported by the Marie Curie Actions-International
256 Outgoing Fellowship (PIOF-GA-2013-629378). We thank the four anonymous reviewers for their
257 suggestions and comments to improve this manuscript.

258 The authors declare no conflict of interest.

259

260 **References**

261 Alonso-Sáez, L., & Gasol, J. M. (2007). Seasonal variations in the contributions of different bacterial
262 groups to the uptake of low-molecular-weight compounds in northwestern Mediterranean coastal
263 waters. *App Environ Microbiol* 73: 3528-3535.

264 Alonso-Sáez, L., Sánchez, O., Gasol, J. M., Balagué, V., & Pedrós-Alio, C. (2008). Winter-to-summer
265 changes in the composition and single-cell activity of near-surface Arctic prokaryotes. *Environ*
266 *Microbiol* 10: 2444-2454.

267 Becker, J. W., Hogle, S. L., Rosendo, K., & Chisholm, S. W. (2019). Co-culture and biogeography of
 268 *Prochlorococcus* and SAR11. *ISMEj*, 13: 1506-1519.

269 Beier, S., Galvez, M.J., Molina, V., Sarthou, G., Qu  rou  , F., Blain, S., and Obernosterer, I. (2015) The
 270 transcriptional regulation of the glyoxylate cycle in SAR11 in response to iron fertilization in the
 271 Southern Ocean. *Environ Microbiol* 7: 427-434.

272 Bertrand, E.M., Saito, M.A., Rose, J.M., Riesselman, C.R., Lohan, M.C., Noble, A.E. *et al.* (2007)
 273 Vitamin B-12 and iron colimitation of phytoplankton growth in the Ross Sea. *Limnology and*
 274 *Oceanography* 52: 1079-1093.

275 Blain, S., Capparos, J., Gu  neugu  s, A., Obernosterer, I., and Oriol, L. (2015) Distributions and
 276 stoichiometry of dissolved nitrogen and phosphorus in the iron-fertilized region near Kerguelen
 277 (Southern Ocean). *Biogeosciences* 12: 623-635.

278 Blain, S., Quegu  ner, B., Armand, L., Belviso, S., Bombled, B., Bopp, L. *et al.* (2007) Effect of natural
 279 iron fertilization on carbon sequestration in the Southern Ocean. *Nature* 446: 1070-1010U1071.

280 Brown, M.V., Lauro, F.M., DeMaere, M.Z., Muir, L., Wilkins, D., Thomas, T. *et al.* (2012) Global
 281 biogeography of SAR11 marine bacteria. *Molecular Systems Biology* 8.

282 Caporaso, J.G., Bittinger, K., Bushman, F.D., DeSantis, T.Z., Andersen, G.L., and Knight, R. (2010a)
 283 PyNAST: a flexible tool for aligning sequences to a template alignment. *Bioinformatics* 26: 266-
 284 267.

285 Caporaso, J.G., Kuczynski, J., Stombaugh, J., Bittinger, K., Bushman, F.D., Costello, E.K. *et al.*
 286 (2010b) QIIME allows analysis of high-throughput community sequencing data. *Nature Methods* 7:
 287 335-336.

288 Carlson, C.A., Morris, R., Parsons, R., Treusch, A.H., Giovannoni, S.J., and Vergin, K. (2009)
 289 Seasonal dynamics of SAR11 populations in the euphotic and mesopelagic zones of the
 290 northwestern Sargasso Sea. *ISME J* 3: 283-295.

291 Christaki, U., Lefèvre, D., Georges, C., Colombet, J., Catala, P., Courties, C. *et al.* (2014) Microbial
 292 food web dynamics during spring phytoplankton blooms in the naturally iron-fertilized Kerguelen
 293 area (Southern Ocean). *Biogeosciences* 11: 6739-6753.

294 Church, M. J., Hutchins, D. A., and Ducklow, H. W. (2000) Limitation of bacterial growth by
 295 dissolved organic matter and iron in the Southern Ocean. *App Environ Microbiol* 66: 455-466.

296 Debeljak, P., Toulza, E., Beier, S., Blain, S., and Obernosterer, I. (2019) Microbial iron metabolism as
 297 revealed by gene expression profiles in contrasted Southern Ocean regimes. *Environ Microbiol.*

298 Delmont, T. O., Kiefl, E., Kilinc, O., Esen, O. C., Uysal, I., Rappe, M. S. et al. (2019). Single-amino
 299 acid variants reveal evolutionary processes that shape the biogeography of a global SAR11
 300 subclade. *Elife* 8: e46497.

301 Eiler, A., Hayakawa, D.H., Church, M.J., Karl, D.M., and Rappe, M.S. (2009) Dynamics of the SAR11
 302 bacterioplankton lineage in relation to environmental conditions in the oligotrophic North Pacific
 303 subtropical gyre. *Environ Microbiol* 11: 2291-2300.

304 Elifantz, H., Malmstrom, R. R., Cottrell, M. T., & Kirchman, D. L. (2005). Assimilation of
 305 polysaccharides and glucose by major bacterial groups in the Delaware Estuary. *App Environ*
 306 *Microbiol* 71: 7799-7805.

307 Field, K., Gordon, D., Wright, T., Rappe, M., Urback, E., Vergin, K., and Giovannoni, S. (1997)
 308 Diversity and depth-specific distribution of SAR11 cluster rRNA genes from marine planktonic
 309 bacteria. *App Environ Microbiol* 63: 63-70.

310 Fourquez, M., Beier, S., Jongmans, E., Hunter, R., and Obernosterer, I. (2016) Uptake of Leucine,
 311 Chitin, and Iron by Prokaryotic Groups during Spring Phytoplankton Blooms Induced by Natural
 312 Iron Fertilization off Kerguelen Island (Southern Ocean). *Front Mar Sci* 3.

313 Giebel, H.-A., Brinkhoff, T., Zwisler, W., Selje, N., and Simon, M. (2009) Distribution of Roseobacter
 314 RCA and SAR11 lineages and distinct bacterial communities from the subtropics to the Southern
 315 Ocean. *Environ Microbiol* 11: 2164-2178.

316 Giovannoni, S.J. (2017) SAR11 Bacteria: The Most Abundant Plankton in the Oceans. *Annual Review*
 317 *of Marine Science* 9.

318 Giovannoni, S.J., Britschgi, T.B., Moyer, C.L., and Field, K.G. (1990) Genetic diversity in Sargasso
 319 Sea bacterioplankton. *Nature* 345: 60-63.

320 Grote, J., Thrash, J.C., Huggett, M.J., Landry, Z.C., Carini, P., Giovannoni, S.J., and Rappe, M.S.
 321 (2012) Streamlining and Core Genome Conservation among Highly Divergent Members of the
 322 SAR11 Clade. *Mbio* 3.

323 Halsey, K. H., Giovannoni, S. J., Graus, M., Zhao, Y., Landry, Z., Thrash, J. C. *et al.* (2017).
 324 Biological cycling of volatile organic carbon by phytoplankton and bacterioplankton. *Limnol*
 325 *Oceanogr* 62: 2650-2661.

326 Hansell, D.A. (2013) Recalcitrant dissolved organic carbon fractions. *Annual review of marine science*
 327 5: 421-445.

328 Haro - Moreno, J.M., Rodriguez - Valera, F., Rosselli, R., Martinez - Hernandez, F., Roda - Garcia,
 329 J.J., Gomez, M.L. *et al.* (2020) Ecogenomics of the SAR11 clade. *Environ Microbiol* 22: 1748-
 330 1763.

331 Hernandez-Magana, A.E., Liu, Y., Debeljak, P., Crispi, O., Marie, B., Koedooder, C., and
 332 Obernosterer, I. (2021) Prokaryotic diversity and activity in contrasting productivity regimes in late
 333 summer in the Kerguelen region (Southern Ocean). *Journal of Marine Systems* 221: 103561.
 334 Hogle, S.L., Thrash, J.C., Dupont, C.L. and Barbeau, K.A. (2016) Trace metal acquisition by marine
 335 heterotrophic bacterioplankton with contrasting trophic strategies. *App Environ Microbiol* 82:
 336 1613-1624.
 337 Hopkinson, B.M., and Barbeau, K.A. (2012) Iron transporters in marine prokaryotic genomes and
 338 metagenomes. *Environmental microbiology* 14: 114-128.
 339 Jimenez-Infante, F., Ngugi, D.K., Vinu, M., Blom, J., Alam, I., Bajic, V.B., and Stingl, U. (2017)
 340 Genomic characterization of two novel SAR11 isolates from the Red Sea, including the first strain
 341 of the SAR11 Ib clade. *FEMS Microbiol Ecol* 93: fix083.
 342 Kraemer, S., Ramachandran, A., Colatriano, D., Lovejoy, C., and Walsh, D. (2019) Diversity,
 343 biogeography, and evidence for endemism of SAR11 bacteria from the Arctic Ocean. *bioRxiv*:
 344 517433.
 345 Laghdass, M., Catala, P., Caparros, J., Oriol, L., Lebaron, P., and Obernosterer, I. (2012) High
 346 Contribution of SAR11 to Microbial Activity in the North West Mediterranean Sea. *Microbial Ecol*
 347 63: 324-333.
 348 Landa, M., Blain, S., Christaki, U., Monchy, S., and Obernosterer, I. (2016) Shifts in bacterial
 349 community composition associated with increased carbon cycling in a mosaic of phytoplankton
 350 blooms. *ISME J* 10: 39-50.

351 Landa, M., Blain, S., Harmand, J., Monchy, S., Rapaport, A., and Obernosterer, I. (2018) Major
 352 changes in the composition of a Southern Ocean bacterial community in response to diatom-derived
 353 dissolved organic matter. *FEMS Microbiol Ecol* 94.

354 Lasbleiz, M., Leblanc, K., Armand, L.K., Christaki, U., Georges, C., Obernosterer, I., and Quéguiner,
 355 B. (2016) Composition of diatom communities and their contribution to plankton biomass in the
 356 naturally iron-fertilized region of Kerguelen in the Southern Ocean. *FEMS Microbiol Ecol* 92.

357 Liu, Y., Debeljak, P., Rembauville, M., Blain, S., and Obernosterer, I. (2019) Diatoms shape the
 358 biogeography of heterotrophic prokaryotes in early spring in the Southern Ocean. *Environmental*
 359 *Microbiology* 21: 1452-1465.

360 Liu, Y., Blain, S., Crispi, O., Rembauville, M., and Obernosterer, I. (2020) Seasonal dynamics of
 361 prokaryotes and their associations with diatoms in the Southern Ocean as revealed by an
 362 autonomous sampler. *Environmental Microbiology* 22: 3968-3984.

363 Malmstrom, R.R., Kiene, R.P., Cottrell, M.T., and Kirchman, D.L. (2004) Contribution of SAR11
 364 bacteria to dissolved dimethylsulfoniopropionate and amino acid uptake in the North Atlantic
 365 ocean. *App Environ Microbiol* 70: 4129-4135.

366 Malmstrom, R.R., Cottrell, M.T., Elifantz, H., and Kirchman, D.L. (2005) Biomass production and
 367 assimilation of dissolved organic matter by SAR11 bacteria in the Northwest Atlantic Ocean. *App*
 368 *Environ Microbiol* 71: 2979-2986.

369

370 McDonald, D., Price, M.N., Goodrich, J., Nawrocki, E.P., DeSantis, T.Z., Probst, A. *et al.* (2012) An
 371 improved Greengenes taxonomy with explicit ranks for ecological and evolutionary analyses of
 372 bacteria and archaea. *ISME J* 6: 610-618.

373

374 Moore, E. R., Davie-Martin, C. L., Giovannoni, S. J., & Halsey, K. H. (2020). Pelagibacter metabolism
375 of diatom-derived volatile organic compounds imposes an energetic tax on photosynthetic carbon
376 fixation. *Environ Microbiol* 22: 1720-1733.

377 Moore, E. R., Weaver, A. J., Davis, E. W., Giovannoni, S. J., & Halsey, K. H. (2022). Metabolism of
378 key atmospheric volatile organic compounds by the marine heterotrophic bacterium *Pelagibacter*
379 HTCC1062 (SAR11). *Environ Microbiol* 24: 212-222.

380 Morris, R.M., Rappe, M.S., Connon, S.A., Vergin, K.L., Siebold, W.A., Carlson, C.A., and
381 Giovannoni, S.J. (2002) SAR11 clade dominates ocean surface bacterioplankton communities.
382 *Nature* 420: 806-810.

383 Morris, R.M., Frazar, C., and Carlson, C.A. (2012) Basin-scale patterns in the abundance of SAR11
384 subclades, marine *Actinobacteria* (OM1), members of the *Roseobacter* clade and OCS116 in the
385 South Atlantic. *Environ Microbiol* 14: 1133-1144.

386 Ngugi, D.K., and Stingl, U. (2012) Combined Analyses of the ITS Loci and the Corresponding 16S
387 rRNA Genes Reveal High Micro- and Macrodiversity of SAR11 Populations in the Red Sea. *PLOS*
388 *ONE* 7: e50274.

389 Obernosterer, I., Catala, P., Lebaron, P., and West, N.J. (2011) Distinct bacterial groups contribute to
390 carbon cycling during a naturally iron fertilized phytoplankton bloom in the Southern Ocean.
391 *Limnol Oceanogr* 56: 2391-2401.

392 Obernosterer, I., Fourquez, M., and Blain, S. (2015) Fe and C co-limitation of heterotrophic bacteria in
393 the naturally fertilized region off the Kerguelen Islands. *Biogeosciences* 12: 1983-1992.

394 Ortmann, A.C., and Santos, T.T. (2016) Spatial and temporal patterns in the Pelagibacteraceae across
 395 an estuarine gradient. *FEMS Microbiol Ecol* 92: fiw133.

396 Park, Y.H., Durand, I., Kestenare, E., Rougier, G., Zhou, M., d'Ovidio, F. *et al.* (2014) Polar Front
 397 around the Kerguelen Islands: An up-to-date determination and associated circulation of
 398 surface/subsurface waters. *Journal of Geophysical Research-Oceans* 119: 6575-6592.

399 Pollard, R.T., Salter, I., Sanders, R.J., Lucas, M.I., Moore, C.M., Mills, R.A. *et al.* (2009) Southern
 400 Ocean deep-water carbon export enhanced by natural iron fertilization. *Nature* 457: 577.

401 Quast, C., Pruesse, E., Yilmaz, P., Gerken, J., Schweer, T., Yarza, P. *et al.* (2013) The SILVA
 402 ribosomal RNA gene database project: improved data processing and web-based tools. *Nucleic
 403 Acids Research* 41: D590-D596.

404 Qu  rou  , F., Sarthou, G., Planquette, H.F., Bucciarelli, E., Chever, F., van der Merwe, P. *et al.* (2016)
 405 High variability in dissolved iron concentrations in the vicinity of the Kerguelen Islands (Southern
 406 Ocean). *Biogeosciences* 12: 3869-3883.

407 Rappe, M.S., Connon, S.A., Vergin, K.L., and Giovannoni, S.J. (2002) Cultivation of the ubiquitous
 408 SAR11 marine bacterioplankton clade. *Nature* 418: 630-633.

409 Ruiz-Perez, C.A., Bertagnolli, A.D., Tsementzi, D., Woyke, T., Stewart, F.J. and Konstantinidis, K.T.
 410 (2021) Description of *Candidatus Mesopelagibacter carboxydoxydans* and *Candidatus*
 411 *Anoxipelagibacter denitrificans*: Nitrate-reducing SAR11 genera that dominate mesopelagic and
 412 anoxic marine zones. *Syst Appl Microb* 44: 126185.

413 Salter, I., Galand, P.E., Fagervold, S.K., Lebaron, P., Obernosterer, I., Oliver, M.J. *et al.* (2014)
 414 Seasonal dynamics of active SAR11 ecotypes in the oligotrophic Northwest Mediterranean Sea.
 415 *ISME J* 9: 347-360.

416 Smith, D. P., Kitner, J. B., Norbeck, A. D., Clauss, T. R., Lipton, M. S., Schwalbach, M. S. *et al.*
 417 (2010). Transcriptional and translational regulatory responses to iron limitation in the globally
 418 distributed marine bacterium *Candidatus Pelagibacter ubique*. PLoS One 5: e10487.
 419 Sow, S.L., Brown, M.V., Clarke, L.J., Bissett, A., van de Kamp, J., Trull, T.W. *et al.* (2022)
 420 Biogeography of Southern Ocean prokaryotes: a comparison of the Indian and Pacific
 421 sectors. Environ Microbiol 24: 2449-2466.
 422 Straza, T. R., Ducklow, H. W., Murray, A. E., & Kirchman, D. L. (2010). Abundance and single-cell
 423 activity of bacterial groups in Antarctic coastal waters. Limnol Oceanogr 55: 2526-2536.
 424 Sun, J., Steindler, L., Thrash, J. C., Halsey, K. H., Smith, D. P., Carter, A. E. *et al.* (2011). One carbon
 425 metabolism in SAR11 pelagic marine bacteria. PloS one 6: e23973.
 426 Sun, Y., Debeljak, P., and Obernosterer, I. (2021) Microbial iron and carbon metabolism as revealed by
 427 taxonomy-specific functional diversity in the Southern Ocean. The ISME Journal 15: 2933-2946.
 428 Sunagawa, S., Coelho, L.P., Chaffron, S., Kultima, J.R., Labadie, K., Salazar, G. *et al.* (2015) Structure
 429 and function of the global ocean microbiome. Science 348: 1261359.
 430 Tada, Y., Makabe, R., Kasamatsu-Takazawa, N., Taniguchi, A., and Hamasaki, K. (2013) Growth and
 431 distribution patterns of *Roseobacter/Rhodobacter*, SAR11, and *Bacteroidetes* lineages in the
 432 Southern Ocean. Polar Biology 36: 691-704.
 433 Tamura, K., Stecher, G., Peterson, D., Filipski, A., and Kumar, S. (2013) MEGA6: Molecular
 434 Evolutionary Genetics Analysis Version 6.0. Molecular Biology and Evolution 30: 2725-2729.
 435 Thrash, J.C., Temperton, B., Swan, B.K., Landry, Z.C., Woyke, T., DeLong, E.F. *et al.* (2014) Single-
 436 cell enabled comparative genomics of a deep ocean SAR11 bathytype. ISME J 8: 1440-1451.

437 Tremblay, L., Caparros, J., Leblanc, K., and Obernosterer, I. (2015) Origin and fate of particulate and
 438 dissolved organic matter in a naturally iron-fertilized region of the Southern Ocean. *Biogeosciences*
 439 12: 607-621.

440 Tsementzi, D., Wu, J., Deutsch, S., Nath, S., Rodriguez-R, L.M., Burns, A.S. *et al.* (2016) SAR11
 441 bacteria linked to ocean anoxia and nitrogen loss. *Nature* 536: 179-183.

442 Tucker, S. J., Freel, K. C., Monaghan, E. A., Sullivan, C. E., Ramfelt, O., Rii, Y. M., & Rappé, M. S.
 443 (2021). Spatial and temporal dynamics of SAR11 marine bacteria across a nearshore to offshore
 444 transect in the tropical Pacific Ocean. *PeerJ*, 9, e12274.

445 Vergin, K.L., Beszteri, B., Monier, A., Thrash, J.C., Temperton, B., Treusch, A.H. *et al.* (2013) High-
 446 resolution SAR11 ecotype dynamics at the Bermuda Atlantic Time-series Study site by
 447 phylogenetic placement of pyrosequences. *ISME J* 7: 1322-1332.

448 Wang, Q., Garrity, G.M., Tiedje, J.M., and Cole, J.R. (2007) Naive Bayesian classifier for rapid
 449 assignment of rRNA sequences into the new bacterial taxonomy. *App Environ Microbiol* 73: 5261-
 450 5267.

451 West, N.J., Obernosterer, I., Zemb, O., and Lebaron, P. (2008) Major differences of bacterial diversity
 452 and activity inside and outside of a natural iron-fertilized phytoplankton bloom in the Southern
 453 Ocean. *Environ Microbiol* 10: 738-756.

454 West, N.J., Lepère, C., Manes, C-LO., Catala, P., Scanlan, D.J. and Lebaron, P. (2016) Distinct Spatial
 455 Patterns of SAR11, SAR86 and Actinobacteria diversity along a transect in the ultra-oligotrophic
 456 South Pacific Ocean. *Front Microbiol* 7:234.

457

Table 1: SAR11 clade contribution to bacterial abundance and bacterial leucine incorporation. Station R-2 represents the HNLC site while A3-2, F-L and E-5 represent Fe-fertilized sites at various bloom development stages (see Figure S1 and Table S1). Data are from this study unless specified, with * indicating surface data previously published in Fourquez *et al.* (2016). n.a.: not available. The percentage of active SAR11 was assessed by leucine uptake through Micro-CARD-FISH. The details of the method are described in (Fourquez *et al.*, 2016). Briefly, 10 mL of seawater samples were incubated with radiolabeled leucine for 6-8h, fixed with paraformaldehyde and filtered onto 0.2 µm polycarbonate filters. The abundance of SAR11 was determined with catalyzed reporter deposition fluorescence in situ hybridization (CARD-FISH) with the probes SAR11-152R, SAR11-441R, SAR11-542R and SAR11-732R (Morris *et al.*, 2002). The micro-autoradiography development with photographic emulsion was exposed for 2-3d. After development the proportion of substrate active SAR11 were determined as the proportion of probe positive cell with silver grains.

Station	Depth (m)	BA ⁽¹⁾ (x10 ⁵ cells ml ⁻¹)	% of BA cells as SAR11 ⁽²⁾	SAR11 abundance (x 10 ⁴ cells ml ⁻¹)	% of active SAR11 ⁽³⁾ cells	% of total active cells as SAR11	% relative abundance of SAR11 OTUs ⁽⁴⁾
R-2	20	2.30	49 ± 7*	11.2	51 ± 9*	60 ± 5	47
R-2	60	2.95	42 ± 4	12.4	38 ± 5	50 ± 3	n.a.
R-2	150	2.87	42 ± 2	12.1	42 ± 3	65 ± 6	14
R-2	300	1.30	19 ± 0	2.47	15 ± 3	23 ± 4	13
A3-2	20	2.70	35 ± 12*	9.45	12 ± 3*	52 ± 10	36
A3-2	80	3.53	43 ± 1	15.2	84 ± 3	58 ± 2	39

A3-2	160	3.47	34 ± 1	11.2	58 ± 9	21 ± 6	41
A3-2	300	1.90	20 ± 3	3.80	30 ± 6	28 ± 4	24
F-L	20	6.06	46 ± 6*	27.9	37 ± 8*	55 ± 5	31
F-L	70	6.48	34 ± 2	22.0	24 ± 4	50 ± 5	41
F-L	150	2.24	11 ± 14	2.46	3 ± 3	13 ± 8	34
F-L	300	1.81	5 ± 9	0.91	0 ± 1	0	19
E-5	20	4.60	34 ± 5*	15.6	60 ± 9*	45 ± 7	n.a.
E-5	80	4.56	36 ± 6	16.4	11 ± 4	58 ± 7	11
E-5	150	3.57	27 ± 3	9.64	25 ± 7	51 ± 3	42
E-5	300	2.20	8 ± 2	1.76	1 ± 1	4 ± 2	22

⁽¹⁾BA: Bacterial abundance determined by flow cytometry (data as published in Christaki *et al.*, 2014)

⁽²⁾ Positive cells hybridized with SAR11 clade probes (*: marks 20 m depth data published in Fourquez *et al.*, 2016)

⁽³⁾Micro-autoradiography positive cells showing leucine incorporation (*: marks 20 m depth data published in Fourquez *et al.*, 2016)

⁽⁴⁾Based on 16s rDNA sequencing (the community-level analysis of the 16S sequencing data from 20m-depth samples can be found in Landa *et al.*, 2016)

Figure legends

Figure 1: Relative abundance (%) of the main bacterial taxonomic groups over the three depth layers. A total of 31 samples from eight different stations were analyzed for bacterial community composition by 454 pyrosequencing of the V1-V3 regions of the 16S rRNA gene. Each bar shows the average contribution of the specified groups across: 12, 11, 8 samples for the mixed, intermediate and deep layer respectively. Filtration, extraction, sequencing procedures and denoising of the sequences are described in [Landa et al. \(2016\)](#). Clean reads were subsequently processed using the Quantitative Insight Into Microbial Ecology pipeline (QIIME v1.7; [\(Caporaso et al., 2010b\)](#)). Reads were clustered into (OTUs) at 99% pairwise identity using Uclust and representative sequences from each bacterial OTU were aligned to Greengenes reference alignment using PyNAST ([\(Caporaso et al., 2010a\)](#)). All singletons and operational taxonomic units (OTUs) present in only one sample were removed. Taxonomy assignments were made using the Ribosomal Database Project (RDP) classifier ([\(Wang et al., 2007\)](#)) against the database Greengene 13_8 ([\(McDonald et al., 2012\)](#)) and SILVA 128 ([\(Quast et al., 2013\)](#)). The data were deposited in the Sequence Read Archive (SRA) database under accession number SRP041580.

Figure 2: Contribution of SAR11 clade to total ^3H -leucine incorporating cells versus contribution of SAR11 clade to total bacterial abundance. The solid line indicates a 1:1 relationship.

Figure 3: Phylogenetic relationships of SAR11 OTUs: Maximum likelihood tree of OTUs closely related to SAR11 clade. Only SAR11 OTUs representing more than 0.1% of the total SAR11 reads are included. Reference sequences from previously published SAR11 subclades

identifications are indicated in blue italic. Bootstrap values (n=1000) are indicated at nodes; scale bar represents changes per positions. SAR11 maximum likelihood tree was computed with Mega7 ([Tamura *et al.*, 2013](#)).

Figure 4: Layer distribution of SAR11 subclades (A) and subclades Ia (B): % relative abundance of SAR11 related OTUs representing more than 0.1 % of all SAR11 OTUs. Average of SAR11 relative abundance across all stations are shown, with error bars representing standard deviation between stations.

Figure 5: Vertical distribution of SAR11 subclades under different bloom conditions (integrated weight average of SAR11 relative abundance to total community, note different z scales, Grey line represent the limit of the mixed layer depth).

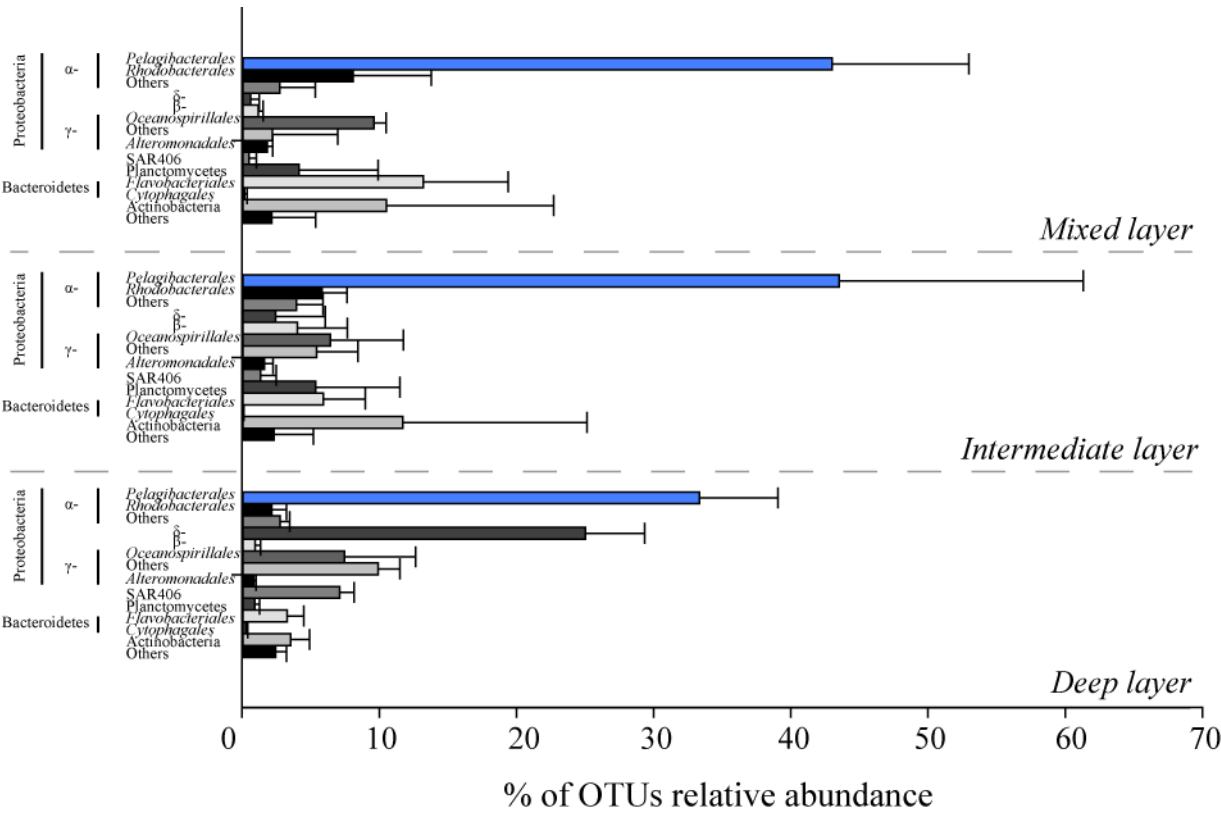


Figure 1

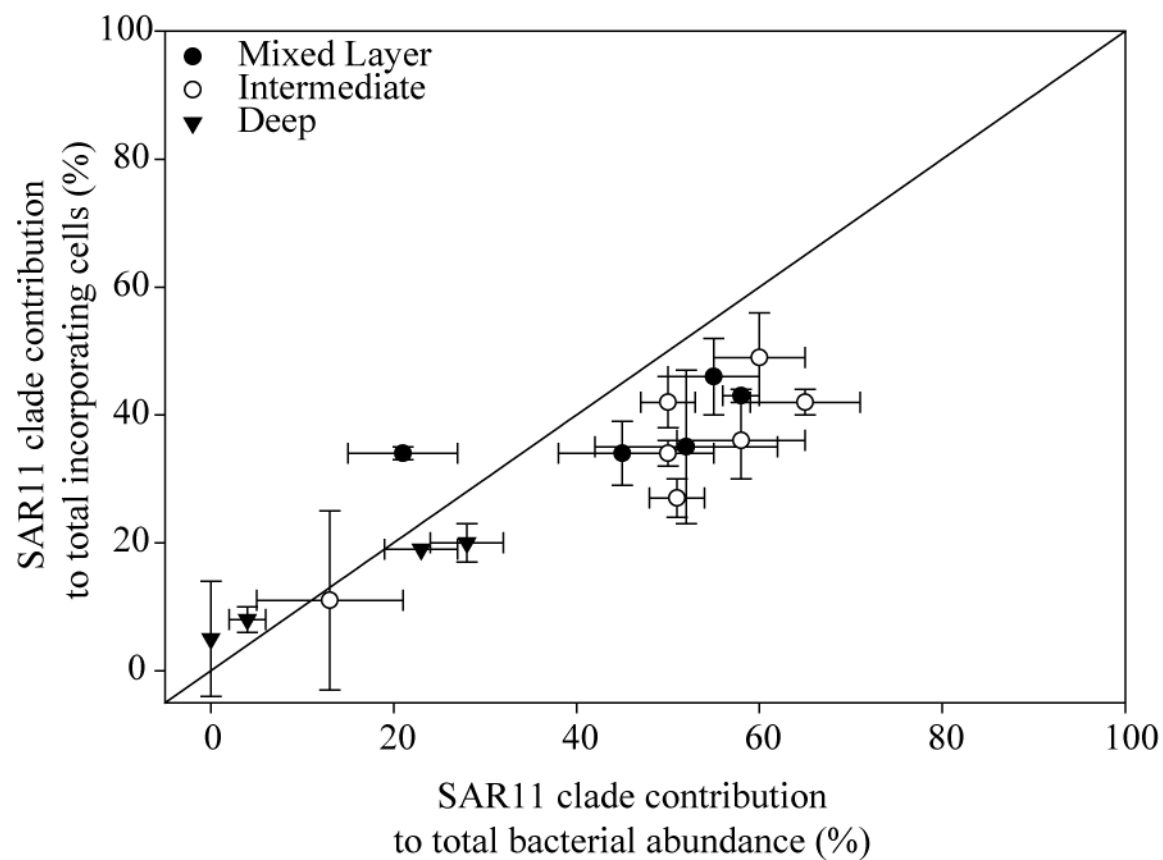


Figure 2

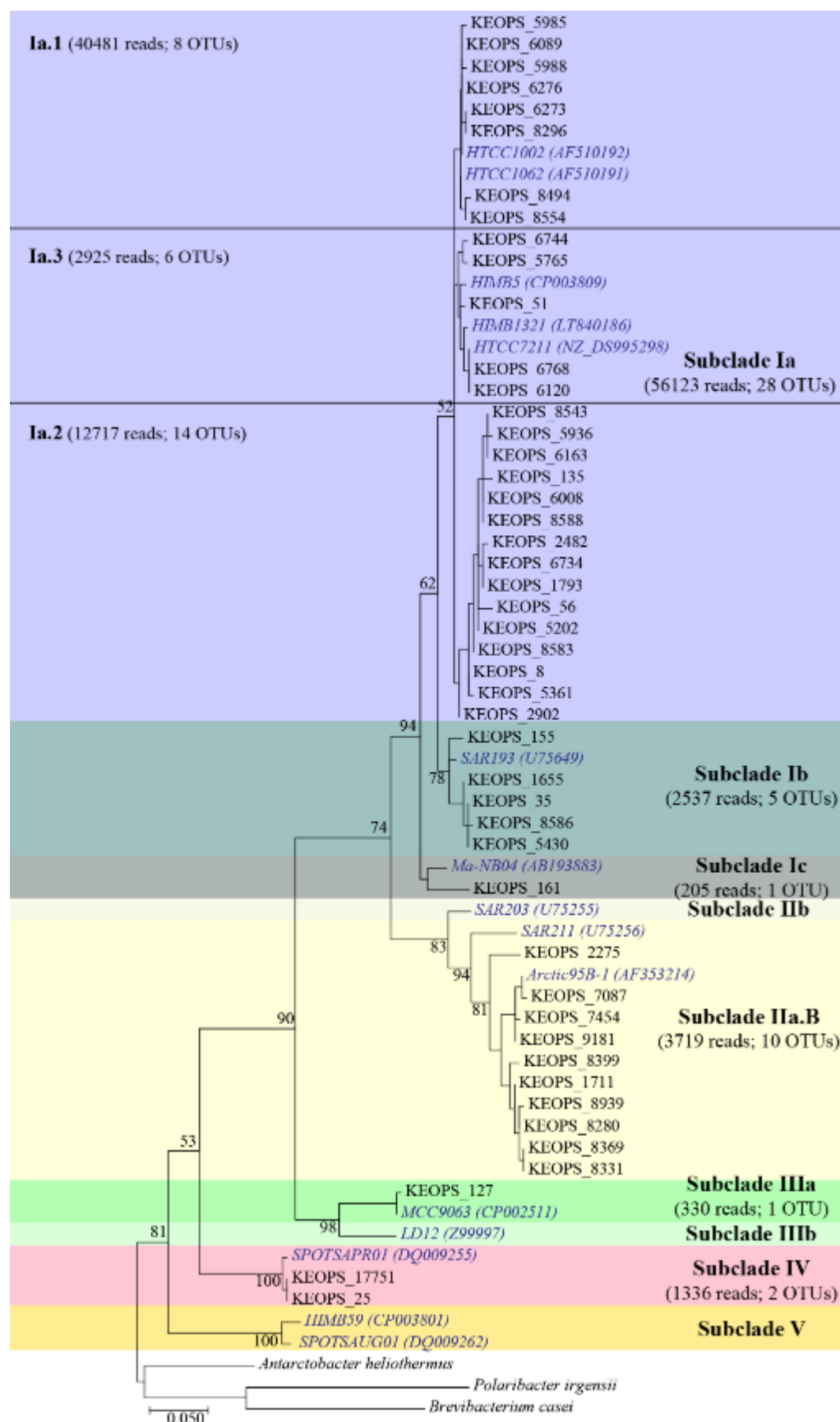


Figure 3

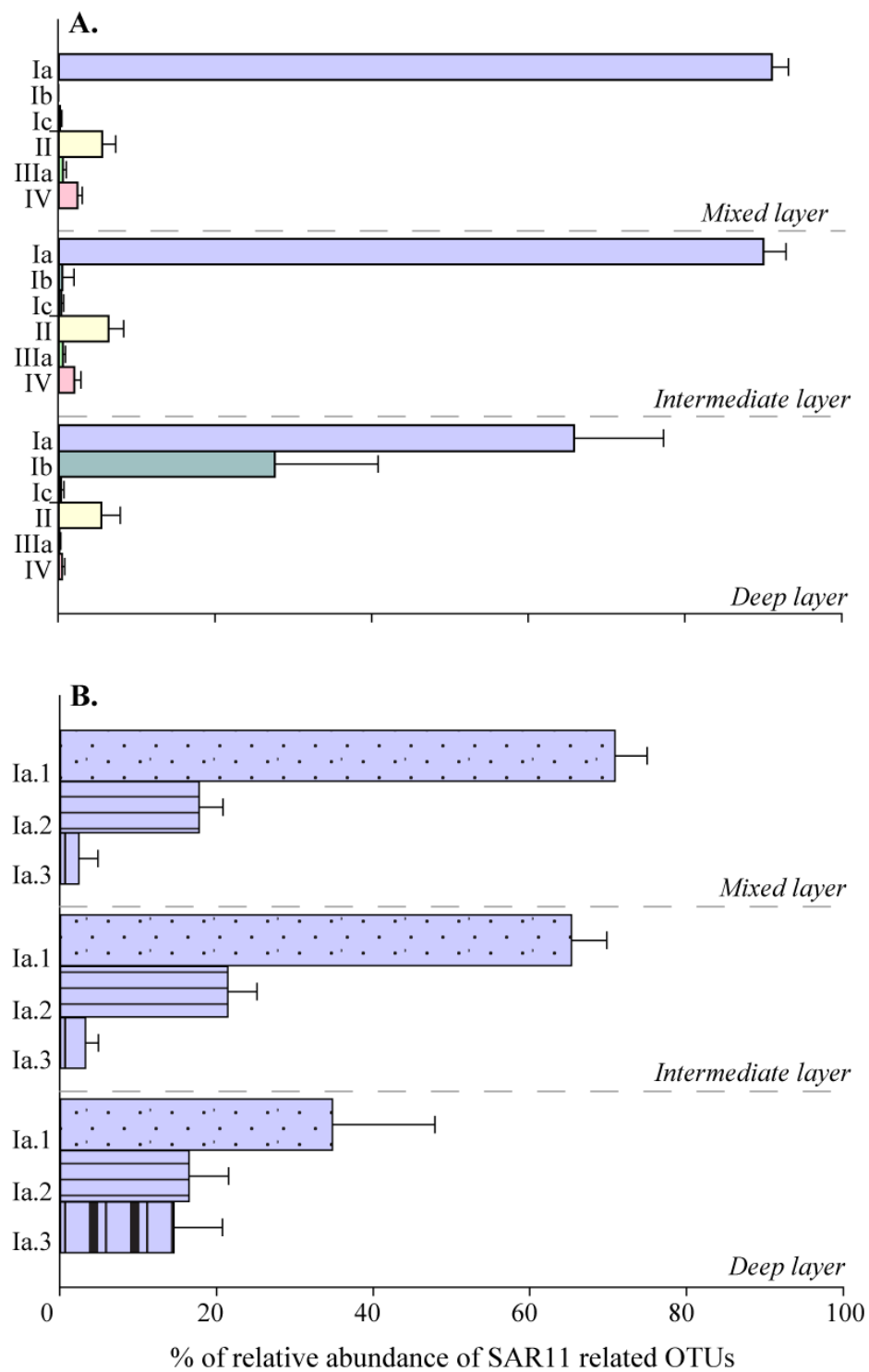


Figure 4

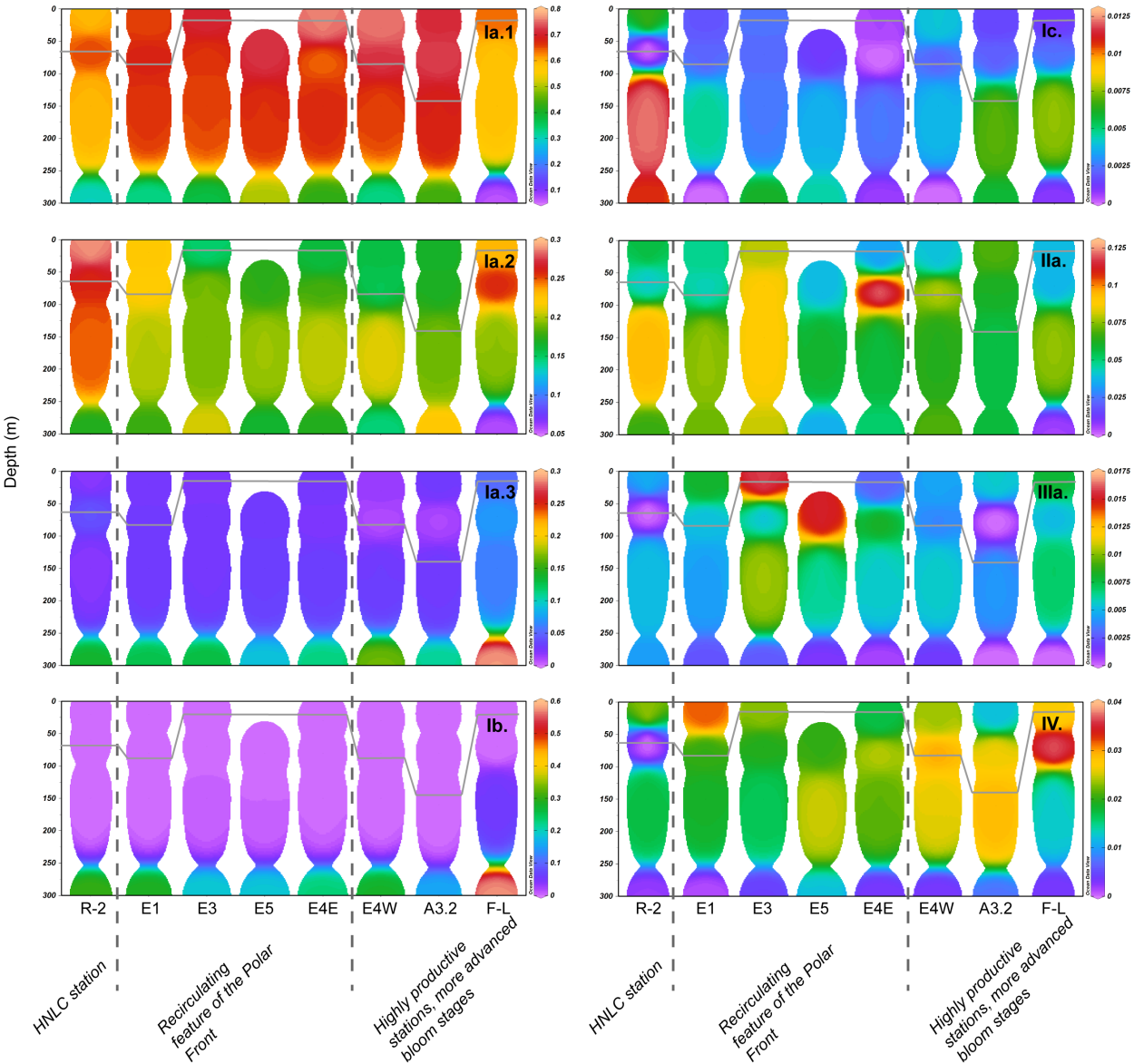


Figure 5

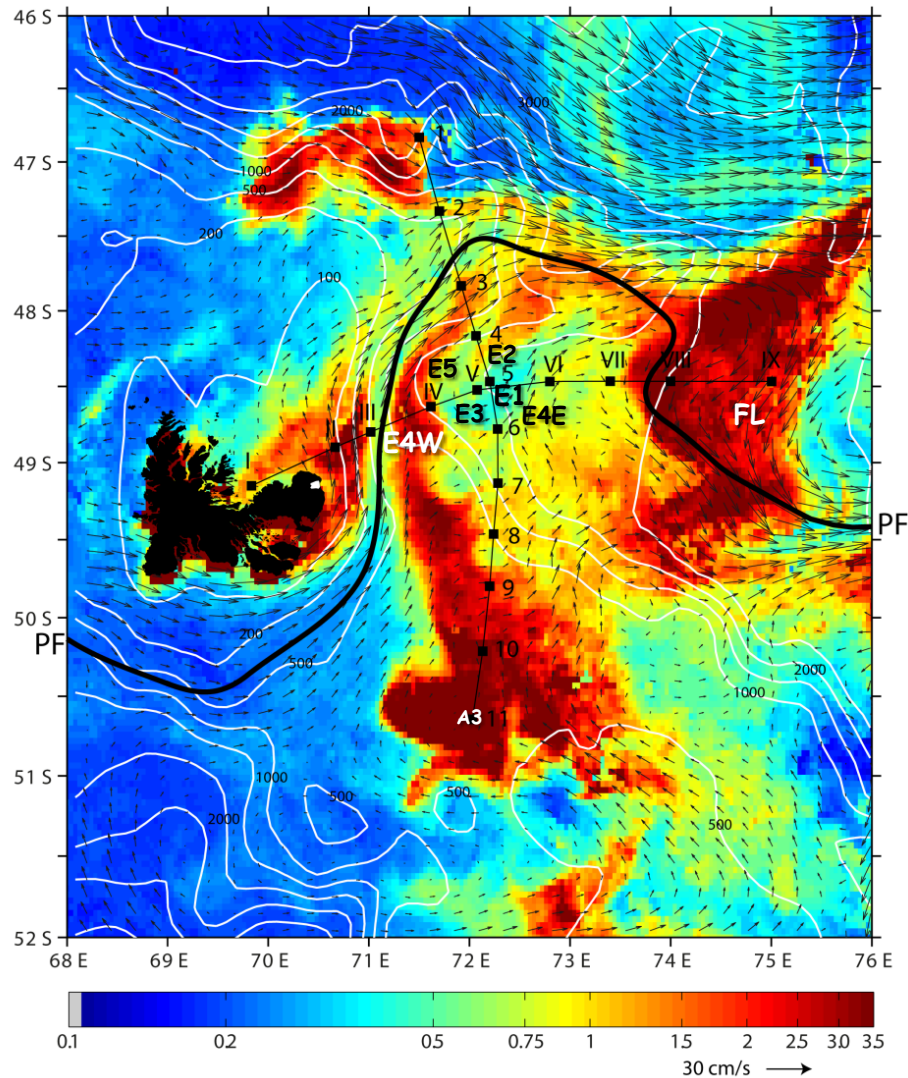
Supplementary Table and Figures

Table S1: Depth layer classification, environmental and bacterial parameters for the sampled stations. (n.a.: not available, HLNC: High nutrients low chlorophyll station). The wind mixed layer depth (MLD) as determined based on a difference in sigma of 0.02 to the surface value, as for instance described in de Boyer Montégut *et al.* (2004). The samples were then attributed to one of the three categories: surface (MLD), intermediate (transition zone between MLD and winter water) and deep (winter water) based on the physical properties as published in Park *et al.* (2014). The sampling was conducted during the KEOPS2 (Kerguelen Ocean and Plateau Compared Study 2) cruise from October to November 2011 on board the R/V Marion Dufresne in the Kerguelen region (FigS1 and see Fig. 1 in Landa *et al.*, 2016). A total of seven stations (A3.2, E stations and F-L) were sampled in the naturally iron-fertilized regions east of the Kerguelen Islands and a reference station (R-2) was sampled in high nutrient low chlorophyll waters (HNLC) located west of the islands. E1, E3, E4-E and E5 were sampled temporally in a quasi-Lagrangian manner. For each station four depths were sampled according to CTD profiles.

Station group	Station	Depth (m)	layer	Chl. <i>a</i> ($\mu\text{g L}^{-1}$)*	Bacterial abundance ($\times 10^5$ cells mL^{-1})*	Bacterial production ($\text{ng C L}^{-1} \text{h}^{-1}$)*
HNLC	R-2	20	Mixed layer	0.32	2.29	2.08
		60	Mixed layer	0.27	2.95	2.77
		150	Intermediate	0.07	2.87	0.88
		300	Deep	-	1.30	0.63
Polar front	F-L	20	Mixed layer	5.12	6.06	64.6
		70	Intermediate	0.34	6.48	6.82
		150	Intermediate	0.04	2.24	1.49
		300	Deep	-	1.81	0.23
Kerguelen Plateau	E4W	30	Mixed layer	1.40	6.04	30.16
		80	Mixed layer	1.22	5.96	24.83

		150	Intermediate	0.22	3.15	4.34
		300	Deep	-	1.76	0.31
Recirculation feature	A3.2	20	Mixed layer	1.65	2.70	20.15
		80	Mixed layer	2.12	3.53	20.63
		160	Mixed layer	2.30	3.47	22.43
		300	Deep	-	1.90	1.09
	E1	20	Mixed layer	1.00	4.33	15.98
		80	Mixed layer	0.85	4.26	14.73
		150	Intermediate	0.60	3.83	9.78
		300	Deep	-	1.34	0.25
	E3	20	Mixed layer	0.69	5.06	23.65
		70	Intermediate	0.42	4.93	16.6
		150	Intermediate	0.50	4.18	9.02
		300	Deep	-	1.81	0.48
	E4E	30	Mixed layer	1.09	5.63	39.65
		80	Intermediate	0.39	5.28	10.97
		150	Intermediate	0.19	3.18	5.06
		300	Deep	-	1.67	0.17
	E5	20	Mixed layer	1.21	4.60	28.27
		80	Intermediate	0.92	4.56	26.43
		150	Intermediate	0.20	3.57	3.3
		300	Deep	-	2.20	0.15

*data from Christaki et al. 2014



Supplementary Figure S1: KEOPS2 study area. The sampling was conducted during the KEOPS2 (Kerguelen Ocean and Plateau Compared Study 2) cruise from October to November 2011 on board the R/V Marion Dufresne in the Kerguelen region (FigS1 and see Fig. 1 in Landa et al., 2016). A total of seven stations (A3.2, E stations and F-L) were sampled in the naturally iron-fertilized regions east of the Kerguelen Islands and a reference station (R-2) was sampled in high nutrient low chlorophyll waters (HNLC) located west of the islands. For each station four depths were sampled according to CTD profiles.

Chl *a* (color scale), surface velocity fields (arrows), the polar front (PF, black line), and the position of the different stations: The Chl *a* rich stations: A3, on the Kerguelen plateau; F-L and E-4W north and south of the polar front; and “E” stations sampled in a quasi-Lagrangian manner (E-1, E-2, E-3, E-4E, and E-5) within a complex meander south of the polar front. The reference HNLC station (R-2) is not shown as it is out of the area of the map (66.692743 E longitude,

50.38954 N latitude). Map is courtesy of Y. Park and colleagues. To note: the chlorophyll content represented on the map corresponds to the last week of the KEOPS2 cruise.

References

- de Boyer Montégut, C., Madec, G., Fischer, A.S., Lazar, A., and Iudicone, D. (2004) Mixed layer depth over the global ocean: An examination of profile data and a profile-based climatology. *J Geophys Res Oceans* 109: C12003.
- Landa, M., Blain, S., Christaki, U., Monchy, S., and Obernosterer, I. (2016) Shifts in bacterial community composition associated with increased carbon cycling in a mosaic of phytoplankton blooms. *ISME J* 10: 39-50.
- Park, Y.H., Durand, I., Kestenare, E., Rougier, G., Zhou, M., d'Ovidio, F. *et al.* (2014) Polar Front around the Kerguelen Islands: An up-to-date determination and associated circulation of surface/subsurface waters. *J Geophys Res Oceans* 119: 6575-6592.